Atom cooling, trapping, and quantum manipulation

Carl E. Wieman

Department of Physics and JILA, National Institute of Standards and Technology, University of Colorado, Boulder, Colorado 80309

David E. Pritchard

Department of Physics, Massachusetts Institute of Technology, Cambridge, Massachusetts 02139

David J. Wineland

National Institute of Standards and Technology, Boulder, Colorado 80303

Neutral atoms and ions can now be cooled, trapped, and precisely manipulated using laser beams and other electromagnetic fields. This has made it possible to control external degrees of freedom at the quantum level, thereby making possible a variety of interesting new physics. [S0034-6861(99)03802-7]

I. INTRODUCTION

Modern atomic, molecular, and optical physics has advanced primarily by using known physics to devise innovative techniques to better isolate and control the atomic system, and then exploiting this nearly ideal system to achieve higher precision and discover new physical phenomena. The striking advances along these lines have been recognized by awards of Nobel Prizes to 21 individuals in this area; most recently, the 1997 Nobel prize was given for laser cooling and trapping of neutral atoms (Phys. Today, 1997). In the first half of the twentieth century, the Stern-Gerlach magnet, and later optical pumping, allowed the preparation and analysis of internal quantum numbers. Resonance techniques allowed the quantum state to be changed controllably, and methods such as Ramsey's separated oscillatory fields, and spin echos created and exploited coherent superposition of internal quantum states. This control of internal states ultimately led to the invention of the maser and the laser. For a brief discussion of what might be called ''Rabi physics,'' see the article by Kleppner in this volume.

This paper discusses the extension of this pattern of control and study to the *external* degrees of freedom (position and velocity) that has occurred in the last few decades. The strong forces of electric and magnetic fields on ions allow them to be trapped with high kinetic energy, and once trapped they can be cooled in various ways. The forces available to trap neutral atoms are much weaker. In order to trap them, they must first be cooled below 1 K by radiation pressure that cannot exceed 1 meV/cm for a strong resonant transition. For cold atoms, trapping has been achieved using resonant radiation pressure and/or forces from field gradients acting on either the atoms' magnetic moments or their induced electric dipole moments. The latter force is produced by the electric field of a near-resonant, tightly focused laser beam. All of these traps have maximum depths, expressed in terms of temperature, on the order of 1 K for practical situations.

Traps, together with cooling methods that have achieved kinetic temperatures as low as nanokelvins, have now created the ultimate physical systems thus far for precision spectroscopy, frequency standards, and tests of fundamental physics. Atomic collisions are qualitatively different, and the cooling has produced new states of matter: ion liquids, crystals, and (neutral) atomic Bose-Einstein condensates. Atoms have been placed in the lowest quantum state of the confining trap potentials, and coherent superpositions of translational states have been created, often entangled with the internal quantum states. These provide novel test beds for quantum mechanics and manipulation of quantum information.

II. MANIPULATING POSITION AND VELOCITY

A. Cooling

Radiation pressure arises from the transfer of momentum when an atom scatters a photon. Radiation pressure cooling uses the Doppler shift with light tuned just below the atomic resonance frequency (Wineland and Itano, 1987; Wieman and Chu, 1989). Atoms that are moving towards the light will see the light Doppler shifted nearer to resonance, and hence will scatter more photons than slower atoms. This slows the faster atoms and compresses the velocity distribution (i.e., cooling the atom sample). A single laser beam is sufficient to cool a sample of trapped atoms or ions; however, free atoms must be irradiated with laser beams from all directions. For atoms with velocities that cause Doppler shifts comparable to the natural transition width (typically several meters per second), this ''optical molasses'' takes just microseconds to cool to the ''Doppler limit.'' This limit is somewhat under 1 mK for a typical, allowed, electric dipole transition.

A variety of methods have been found for cooling isolated atoms and ions to lower temperatures (Wineland and Itano, 1987; Wieman and Chu, 1989; Cohen-Tannoudji and Phillips, 1990). These include sub-Doppler laser cooling, evaporative cooling, and laser ''sideband'' cooling. Sub-Doppler laser cooling uses standing-wave laser beams that give rise to potential energy hills and valleys due to the spatial variations in the atom's ac Stark shift. As an atom moves up a hill, it loses

kinetic energy. Near the top of a hill, optical excitations tend to reorient the atom relative to the local field so that it then sees that location as a potential valley. This efficiently transfers kinetic energy into photon energy, and can cool atoms into the microkelvin range, a few times the recoil energy/temperature gained by the scattering of a single photon. Even lower temperatures can be achieved by evaporative cooling of trapped atoms. The process is analogous to the way a cup of hot coffee cools down by giving off the most energetic molecules as steam. As the energetic atoms are removed from the trap, collisions readjust the remaining atoms into a lower temperature thermal distribution. Trapped atoms have been evaporatively cooled to 50 nK by precisely controlling the removal of the energetic atoms and making traps with very good thermal isolation. Cooling with resolved sidebands (Wineland and Itano, 1987) is a straightforward realization of the principle that a laser transition can simultaneously change the internal and motional quantum states of a trapped atom. For example, if it is sufficiently tightly bound in a harmonic potential, the atom's optical spectrum has resolvable Doppler-effect-generated frequency-modulation sidebands. Absorption on a lower sideband reduces the atom's motional state energy; if the atom's recoil energy is smaller than the motional quanta, overall cooling occurs when the photon is reemitted. This has been used to cool small numbers of trapped ions and atoms to the ground state of the confining potential with high efficiency.

B. Atom optics

Given an ensemble of atoms localized in phase space, a growing cadre of techniques, collectively called ''atom optics,'' have been developed for manipulating atoms with full retention of their quantum coherence (Pritchard, 1991; Adams, Sigel, and Mlynek, 1994). The most salient feature of atom optics is the small size of atomic de Broglie wavelengths relative to optical wavelengths—an order of magnitude smaller for atoms with submillikelvin temperatures, and four orders of magnitude smaller for room-temperature atoms. Preserving atomic coherence for such wavelengths is a major experimental challenge. However, these short wavelengths also suggest that atom optics offers possibilities for precise measurements and subnanometer fabrication. The principal applications of atom optics have been in the creation and use of atom interferometers (Berman, 1997), and for atom lithography—the deposition of precise patterns of atoms on surfaces (Thywissen *et al.*, 1997).

The principle tools of atom optics have been light forces and nanofabricated mechanical structures, and the major technique has been diffraction. If a highly collimated atom wave crosses a standing wave of near-resonant light at right angles, the spatially periodic variation of the light-atom interaction potential energy causes a corresponding variation in the local de Broglie wave number. This diffracts the atom wave like a phase grating in classical optics, where the diffraction orders correspond to the successive absorption and stimulated emission of a pair of photons traveling in opposite directions. The resultant momentum transfer to the atoms is twice the photon momentum. When the atom waves travel through a thick standing wave, one diffracted order predominates. For a thin standing wave, the diffraction pattern is spread over many orders. Blazed gratings have also been demonstrated, as well as Raman and adiabatic-dark-state gratings in which the diffraction is accompanied by a specific change in the internal state of the atoms.

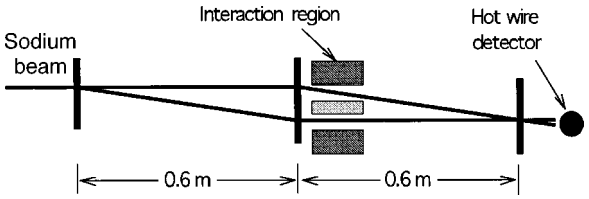

FIG. 1. An example of a three-grating atom interferometer. The sodium beam is split up and then later recombined after the interaction region where the atoms in one arm can be perturbed in various ways. In this example, a hot wire detector detects the fringe pattern.

Mechanical diffractive structures (Keith *et al.*, 1988) differ qualitatively from light gratings. They are purely amplitude gratings (with concomitant loss of intensity), species independent (do not depend on internal structure), and can have periods several times smaller than light. They can be made with arbitrary patterns using electron-beam lithography. Examples include spherical and cylindrical zone plates; a combination of lens and hologram (Morinaga *et al.*, 1996), which produced an atom image with 10^4 resolution elements; and a sieve for ''sizing'' molecules (Luo *et al.*, 1996).

There are no achromatic partially reflecting mirrors for atoms, hence diffraction gratings have been pressed into service as beam splitters and combiners for atom waves. These have been used to make a variety of atom (and even molecule) interferometers since 1991. Nearly all use ''white fringe'' designs that compensate for the dependence of diffraction angle on the wavelength of the individual atoms. A majority have used the three-grating configuration (Fig. 1) in which the first grating splits the incident beam, the second reverses the differential momenta given by the first, and the third recombines the two beams at the location where they overlap. Both mechanical and all types of light gratings have been successfully used. Interference fringes have been read out using both detectors sensitive to atom position and detectors of the atom's internal state.

C. Traps

Trapping atoms can be as simple as putting a gas of atoms in a storage vessel that has walls that inhibit sticking. However, electromagnetic fields can also be configured to confine atoms with much less perturbation to their internal structure and minimal heating from the

surrounding environment (Wieman and Chu, 1989; Ghosh, 1995; Newbury and Wieman, 1996). Although Maxwell's equations put severe constraints on how this can be done (for example, Earnshaw's theorem and its optical analog), numerous clever designs have been found, a few of which are presented here. A very useful trap for neutral atoms is the magnetic bottle. Magnetic substates that are attracted to regions of lower field can be trapped if $|\mathbf{B}|$, and thus the trap potential $U(\mathbf{r})$ have a local minimum. One choice of $\mathbf{B}$ that provides such a potential is a quadrupole field, formed by an ''anti-Helmholtz'' coil (currents in opposite directions in the coils of a Helmholtz pair). This configuration is effective but has the problem that at the center of the coil, the fields vanish. For atoms passing near the center of the coil, the field becomes so small that the magnetic moment alignment is lost with respect to the field direction (''Majorana transitions''), transferring the atoms into untrapped magnetic substrates. A popular choice to overcome this problem has been a trap composed of a linear magnetic quadrupole along whose axis is superimposed an axial field with maxima that ''close'' the ends (the Ioffe-Pritchard configuration). This gives a local, but nonzero minimum in $|\mathbf{B}|$, and hence eliminates the leak in the center.

A trap that works for both neutral and charged atoms relies on the time-averaged force produced by a rapidly oscillating inhomogeneous field. For example, if a charged particle is placed in the center of an oscillating spherical quadrupole field, it is initially pushed outward, taking it to a region of higher field where it will experience a larger push inward when the field has reversed. Thus its micromotion at the field oscillation frequency will cause a nonzero average confining force (the ''ponderomotive force'') that can be described by a pseudopotential. The Paul trap confines atomic ions using this principle. High-energy particle accelerators and storage rings are another form of the ponderomotive force trap, where the oscillating fields arise from the particles traversing inhomogeneous static fields. Induced dipole-moment optical traps rely on the same pondermotive principle. Another trap for charged particles is the Penning ion trap, which uses static electric and magnetic fields. The magnetic field provides confinement normal to this field, while the electric field confines the particles axially along the magnetic field. It is particularly useful for producing large cold samples (see Sec. III.A).

The workhorse of cold neutral atom research is the magneto-optical trap (MOT), because of both its simplicity of construction and its depth (Raab *et al.*, 1987). Radiation pressure from laser beams converging on a center provides the trapping force, but a weak inhomogeneous magnetic field acts as a spatially dependent control on this force. It shifts the magnetic sublevels so that the atoms preferentially absorb the polarized light going toward the trap center. The magnetic field is a spherical quadrupole configuration with gradients of several gauss per centimeter about the zero of the magnetic field, which is the center of the trap. This field has a linear gradient in all three directions, permitting the use of three mutually perpendicular pairs of oppositely circularly polarized laser beams that are detuned a few natural linewidths below a strong atomic transition. Therefore in addition to three-dimensional confinement, the light also provides Doppler and sub-Doppler cooling of the atoms. With only milliwatts of laser power, a typical MOT is 1 K deep, sufficient to capture atoms out of a room-temperature vapor cell.

III. NEW PHYSICS FROM COLD ATOMS

A. One-component plasmas

A collection of trapped ions can be viewed as a ''one-component'' plasma. By cooling such a plasma to very low temperatures, novel liquid and crystalline plasma states have been created (Fig. 2). These crystals can be regarded as the classical limit of Wigner crystallization, where the wave functions of the ions do not overlap and quantum statistics do not play a role. Instead, the crystallization arises entirely from the balance of the trapping fields and the strong long-range Coulomb repulsion between the ions. The structure and formation of these crystals have been studied using Bragg scattering (Itano *et al.*, 1998) and direct imaging of the ions (Walther, 1993; Mitchell *et al.*, 1998).

B. Bose-Einstein condensation in dilute gases

Perhaps the most exciting physics outcome of cooling and trapping techniques has been the creation of a novel macroscopic quantum system, the Bose-Einstein condensate (BEC), in a dilute gas. Bose-Einstein condensate in a gas was first predicted in 1924 (Einstein, 1924, 1925); as a phase transition it is unique because it is driven only by statistics rather than energetics. Superfluid helium, superconductivity, and certain excitation behavior are all manifestations of BEC in various systems. The condensation in a dilute atomic gas was first achieved (Anderson *et al.*, 1995) by cooling a cloud of trapped rubidium atoms so that they were sufficiently cold ($\sim$200 nK) and dense enough that their de Broglie wave packets began to overlap. A large fraction of the atoms then condensed into the ground state of the trapping potential. Bose-Einstein condensate in a gas is proving to be a fascinating new macroscopic quantum system because of the experimental capabilities to manipulate and study it in great detail. Moreover, it is quite amenable to theoretical analysis because the interatomic interactions are relatively weak.

The achievement of BEC (Anderson *et al.*, 1995; Davis *et al.*, 1995) required the combination of many of the techniques for cooling and trapping neutral atoms that had been developed over the previous two decades. It also built on much of the understanding of basic atomic processes at very low temperatures that had been obtained using these techniques. A Bose-Einstein condensate was created (Fig. 3) by first collecting a cloud of laser-cooled atoms in a MOT and cooling them by sub-Doppler laser cooling. At $\sim$10 μK, these were much too

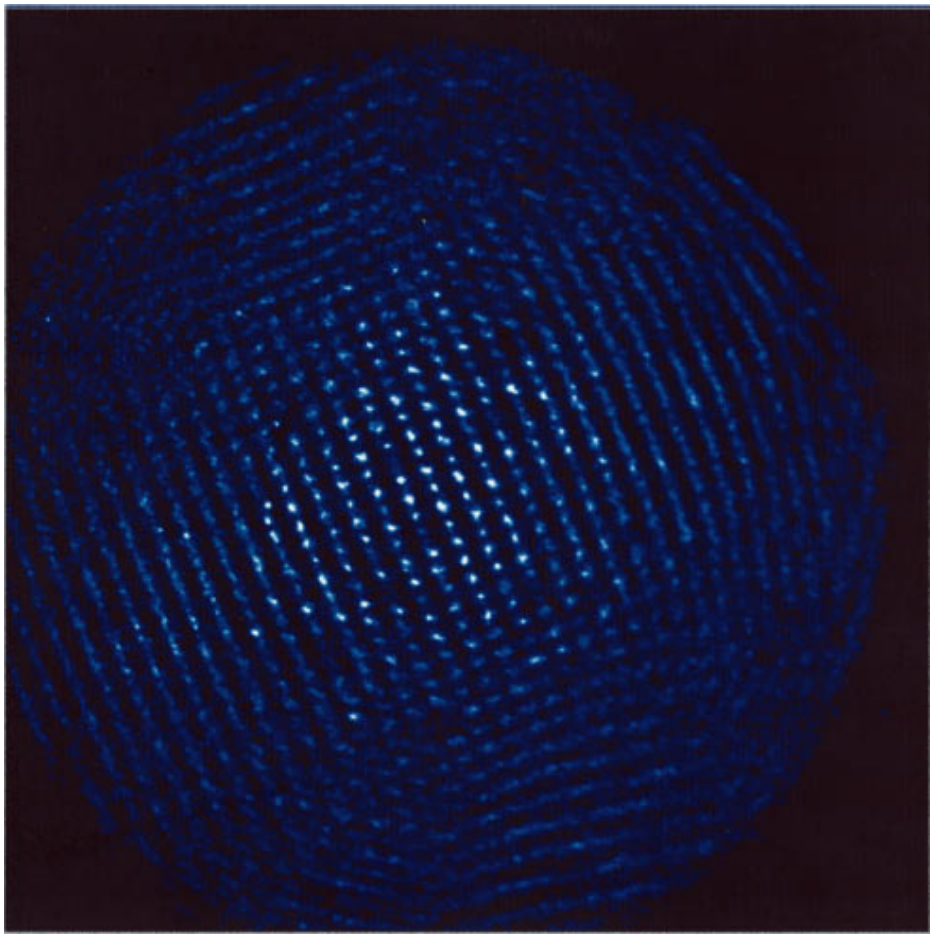

FIG. 2. (Color) Photograph of a large ion crystal. When atomic ions are trapped and cooled, they form crystals whose minimum energy configurations are determined by a balance between the trap potentials and the ions' mutual Coulomb repulsion. In this photograph, about 2000 laser-cooled beryllium ions are confined in a Penning trap. The ion crystal has a BCC configuration with about a 15 μm spacing between ions. As in all Penning traps, the ions rotate about the trap axis (normal to the center of photo) necessitating stroboscopic imaging. (Image courtesy of John Bollinger, NIST.)

hot and dilute for BEC, however. These laser-trapped and cooled atoms were then transferred to a magnetic bottle and evaporatively cooled to below the condensation temperature. Evaporative cooling of magnetically trapped atoms was developed for the pioneering efforts to achieve BEC in gaseous hydrogen (Greytak, 1995). However, it ultimately turned out that laser "precooled" alkali atoms had more favorable collision properties for evaporative cooling (Ketterle and van Druten, 1996). Relative to hydrogen, for every "bad" inelastic collision that causes atoms to be lost from the magnetic trap, there are more "good" thermalizing elastic collisions.[1]

The same convenient optical transitions that provide laser cooling also make it easy to use light scattering to image the cooled alkali clouds and thereby study the condensate. The macroscopic occupation of the ground state that is BEC has been seen both in momentum space, as a peak at zero velocity (Fig. 4), and in real

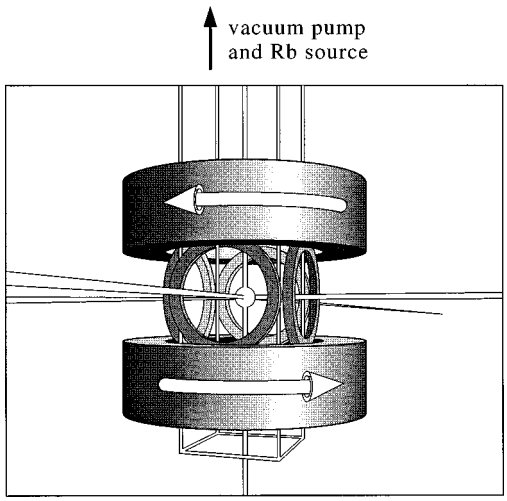

FIG. 3. Schematic of the first apparatus used to create BEC in a dilute gas (Anderson *et al.*, 1995). A room-temperature rectangular glass cell 2.5 cm square by 10 cm high is attached to a vaccum pump and rubidium reservoir (not shown). Light from diode lasers comes from all six directions to form a MOT in the middle of the cell. Running current through the magnetic-field coils shown surrounding the cell creates the magnetic trap.

[1]After the completion of this article, BEC was reported in a gas of spin-polarized hydrogen (D. Kleppner, private communication).

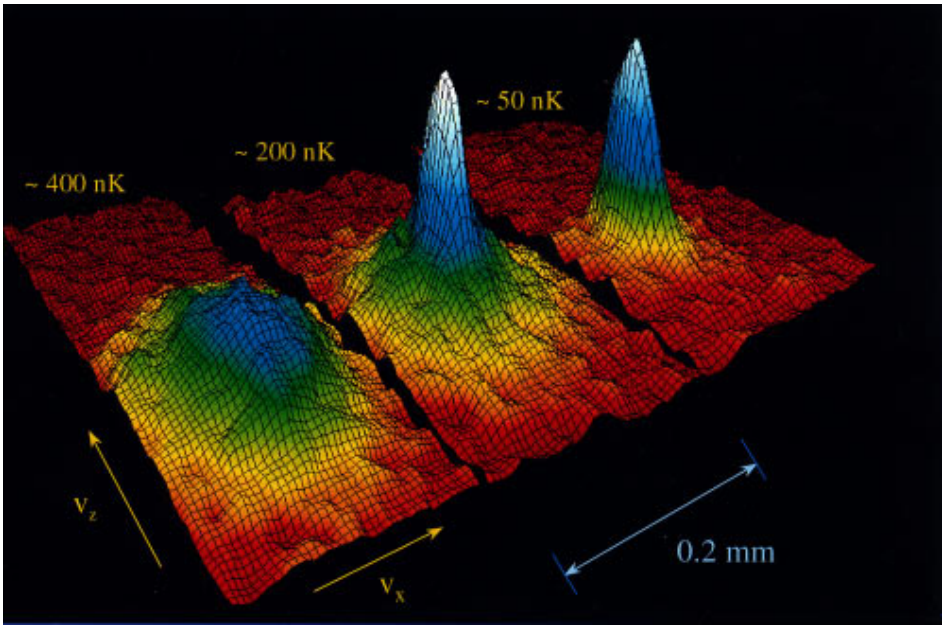

FIG. 4. (Color) Two-dimensional velocity distributions of cold atomic clouds showing BEC. These are for three experimental runs with different amounts of cooling. The axes are the x and z velocities and the number density of atoms. The distribution on the left shows a gentle hill that corresponds to a temperature of about 400 nK. The middle picture is at 200 nK, and shows the asymmetric condensate spire in the center of the hill. The picture on the right is at about 50 nK and about 90% of the atoms are in the condensate. (Courtesy of M. Matthews, University of Colorado.)

space, as a sudden increase in the density of the atoms in the center of the trap. The condensate images provide a unique opportunity for directly observing the shape of a quantum wave function. An advantage of the inhomogeneous trapping potential is that there is spatial separation of condensed and noncondensed portions of the cloud. This makes it possible to distinguish, manipulate, and study the condensed and noncondensed portions of the cloud separately, as well as to create samples of nearly pure condensate. Adding optical fields to the magnetic traps is proving to be a particularly convenient technique to manipulate the condensates and the shape of the confining potential in useful ways (Stamper-Kurn *et al.*, 1998).

There has been an explosion of experimental and theoretical activity in the study of condensates. Initial work considered basic aspects such as the shape of the condensate wave function and how it was distorted by interactions between the atoms. The experimental observations were found to be well described by solutions of the Gross-Pitaevski equation (Gross, 1961, 1963; Pitaevski, 1961) where the self-interaction of the condensate is characterized by a single parameter, the S-wave scattering length. (This is independently measured in cold atom collision experiments.) The validity of this equation has been confirmed over a wide range of interaction strengths by varying the number of atoms in the condensate, and for both positive (repulsive interaction) and negative (attractive interaction) scattering lengths. The fraction of atoms in the condensate and the specific heat, as a function of temperature, have similarly been found to agree very well (within a few percent) with theory.

The dynamical behavior of condensates, including the effects of interactions, has also received considerable study. By modulating the magnetic confining potential, phononlike collective modes of the condensate have been excited. The frequency and damping of these excitations have been studied over a wide range of conditions. For very low temperatures, it was found that the measured resonant frequencies, and their dependencies on the self interaction, agree very precisely with those predicted by the Gross-Pitaevski equation. However, the temperature dependence of the damping and resonant frequencies has proven to be much more difficult to explain theoretically (Jin *et al.*, 1997). These effects, particularly the shifts in frequency, were much larger than simple intuitive models would have suggested, and to explain them requires a more sophisticated treatment of the coupling of condensate and noncondensate phases. This is an area of considerable theoretical and experimental activity.

The various coherence properties of the condensate wave function have been examined in several different ways. The most dramatic was the observation of first-order coherence that occurred when two independent condensates were allowed to pass through each other (Andrews *et al.*, 1997), and the fringes formed in the density distribution as the two-condensate wave functions interfered with each other (Andrews *et al.*, 1997). Third-order coherence (the probability of three-condensate atoms being in the same place) was measured by looking at the rate of three-body recombination in the condensate. This process, in which two atoms bind to form a diatomic molecule and the third atom

carries off energy and momentum, is found to be the dominant process by which atoms are lost from the condensate. It was predicted and then confirmed by experiment that the loss rate would be six times lower in a condensate sample than a noncondensate sample of the same density because of the higher-order coherence of the condensate (a lack of spatial fluctuations in the density).

Among the many other areas of study currently underway or planned, studies of multicomponent condensates appear to be among the richest. The static and dynamical behavior of these interacting quantum fluids can be explored by observing both density and phase of the wave functions. A variety of techniques have been demonstrated for creating multicomponent condensates, and the dynamical evolution of the spatial structure and the phases of the wave functions have been studied in these condensates. These techniques include forming two separate condensates of the same type in a double-well trapping potential, and creating condensates in coherent superpositions of different spin states using radio frequency and microwave magnetic fields.

C. Quantum measurements on single atoms

A single trapped atom affords an opportunity to make repeated measurements on a single quantum system. This provides a display of how an atom will absorb and emit light and exhibit behavior not predicted by the density-matrix formalism which describes ensemble averages. A simple example is an ion with two excited states: one, denoted $|s\rangle$, with strong coupling to the ground state; the other, denoted $|w\rangle$, with weak coupling and a correspondingly long lifetime. If a laser excites the strong transition, strong fluorescence will be observed until the ion is somehow (for example, by spontaneous decay or the action of another laser tuned to the weak transition) transferred to state $|w\rangle$. Then the fluorescence will stop for a time characteristic of the decay time of this state. This behavior is called atom "shelving" and provides a way to tell when the ion is in the $|w\rangle$ state without disturbing it if it is in that state (Fig. 5) (Blatt and Zoller, 1988). Even a single driven two-state atom exhibits interesting correlations: if a fluorescence photon is observed, another photon cannot be emitted for a time on the order of the excited-state lifetime while the excited-state amplitude builds up again. This is called "photon antibunching" and is a purely quantum effect.

D. Quantum-state engineering

Atom manipulation techniques provide a means to synthesize arbitrary and, in general, entangled quantum states from initially unentangled quantum systems (Monroe and Bollinger, 1997). A simple example is an optical beamsplitter in atom interferometry. When a two-level atom (states g and e) is excited by a laser beam directed perpendicular to its motion, a $\pi/2$ pulse creates an entangled state of the form $2^{-1/2}[\Psi(g,0)+\Psi(e,\hbar k)]$ where the second argument denotes the momentum state along the laser beam direction. Thus the atom has states where the momentum is entangled with the internal state. For an atom confined in a harmonic trap, we can create an entangled state of the form $2^{-1/2}[\Psi(g)\Psi(\alpha)+\Psi(e)\Psi(\alpha')]$, where $\Psi(\alpha)$ and $\Psi(\alpha')$ are coherent states—states that are most nearly classical in that they correspond to Gaussian wave packets that oscillate in the trap without changing shape. This state has been created by first optically pumping and laser-cooling a single ion to its internal and motional ground states. Next, the ion's internal state is placed into a coherent superposition state $2^{-1/2}[\Psi(g)+\Psi(e)]$ with resonant radiation. Optical dipole forces that are modulated at the ion's trap oscillation frequency create coherent states of motion. These forces can be applied with two different laser beams whose polarizations are chosen to selectively excite first the state $\Psi(g)$ and then the state $\Psi(e)$ with different modulation phases, with the result that each internal state is associated with a different coherent motional state. When $\Psi(\alpha)$ and $\Psi(\alpha')$ correspond to well-separated, localized spatial wave packets (e.g., oscillations out of phase), this state is called a "Schrödinger-cat" state because a classical-like property (the position) is entangled with a quantum property (the internal state) (Monroe and Bollinger, 1997). Schemes exist to generate arbitrary entangled states between many internal and motional states of an atom. These entangled states can be completely characterized by a family of operations that selectively map different parts of the wave function on to a particular internal state that is then detected—so-called tomographic techniques (Leibfried *et al.*, 1998).

Quantum-state engineering methods can be extended from a single atom to entangled states of many atoms, if a suitable coupling mechanism can be found. The strong Coulomb interaction between cold trapped ions provides one such mechanism. Two ions in the sample can be entangled by first entangling the internal state of one ion with a collective mode of the ions' motion using operations similar to the creation of the Schrödinger cat. This mode, which is *shared* among all ions, could be the

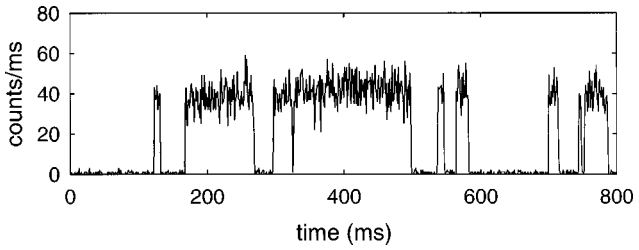

FIG. 5. Quantum jumps. The number of fluorescent photons detected in 0.5 ms sampling times from a trapped and cooled mercury ion. The fluorescence corresponds to laser scattering on the transition between the $6s\ ^2S_{1/2}$ ground state and $6p\ ^2P_{1/2}$ state (level s in the text). With 10^{-7} probability, the $^2P_{1/2}$ state decays to the lower lying ^2D level (level w in text) and fluorescence stops until the ^2D levels decay back to the $^2S_{1/2}$ ground state. By discriminating between fluorescence levels, it is possible to detect the "w" state with nearly 100% efficiency.

center-of-mass mode of motion where all ions oscillate together at the frequency of a single ion as described in the previous paragraph. This mode of motion can then be entangled with a second ion, thereby entangling the internal states of the two selected ions. This can be done in such a way that, at the end, the motional state factors out of the wave function, leaving only the ions' internal states entangled (Cirac and Zoller, 1995).

The ideas of quantum computation have provided a useful framework in which to cast these methods. This is because a general computation can be broken down into a series of elementary operations involving single ion (''qubit'') internal state rotations and a single type of entangling operation between two ions, and because a ''computation'' can always be devised to create an arbitrary entangled state. Quantum computation algorithms have recently been shown to be capable of solving certain problems that are intractable on a classical computer, such as factorization of large numbers (Ekert and Jozsa, 1996; Steane, 1998). These algorithms may remain technically unfeasible in the near future because of the fragility of the entangled states; however, more modest algorithms, such as one for efficiently measuring atomic spectral lines (Bollinger *et al.*, 1996), appear to be within reach. Independent of the outcome of quantum computation, quantum state engineering is allowing detailed studies of the ideas of coherence and decoherence in quantum mechanics (as represented by the fragility of entangled states) and, correspondingly, the capabilities and limits of quantum measurement.

IV. PRECISION MEASUREMENTS

A. Spectroscopy and clocks

Trapping, combined with very low temperatures, can lead to very long observation times and suppression of Doppler effects (including time dilation). This leads to very accurate high-resolution spectroscopy. A classic example is provided by the single electrons (and positrons) trapped in Penning traps, by the group of Dehmelt and van Dyck (Dehmelt, 1995; Ghosh, 1995). These experiments effectively measured the ratio of the electron's spin-flip frequency to its cyclotron resonance frequency in the same magnetic field, thereby determining the g factor of the electron to an inaccuracy of less than 5 parts in 10^{12}. The comparison of this measurement with the value predicted by quantum electrodynamics is the most accurate comparison of the experimental value of a quantity to its theoretical value in all of physics.

Another application of spectroscopy is to atomic clocks, where accurate time intervals are realized by counting cycles of radiation that is exactly in resonance with an atomic transition (Bergquist, 1996). The fundamental limit to the measurement resolution is the duration of the observation time. Major advances have been possible using trapped ions and very cold neutral atoms in ''atomic fountains.'' Now, the world's most precise cesium clocks (which define the second) are based on a cesium fountain. In this device, a sample of 10^6 cold ($\approx$1 μK) cesium atoms is launched upward. The atoms go up 1 m and then fall back toward the source. At both the beginning and the end of their trajectory (1 s apart), the atoms pass through a microwave cavity. Ramsey's method of separated oscillatory fields is used to drive the hyperfine ''clock'' transition ($\approx$9.2 GHz), achieving a linewidth of about 1 Hz. This narrow linewidth, coupled with the relatively small perturbations on the atoms in free flight, has led to a measurement inaccuracy of only 2 parts in 10^{15}, currently the most precise direct measurement of any physical quantity (Simon *et al.*, 1997).

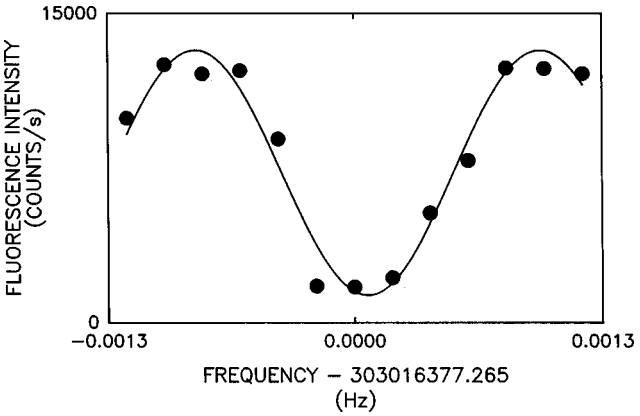

FIG. 6. Atom traps enable long observation times and thus high resolution for atomic clocks. The figure shows a resonance curve for a ground-state hyperfine transition (303 MHz) in laser-cooled beryllium ions that is less than 0.001 Hz wide.

Since the fields in ion traps act on the ions' overall charge and do not significantly perturb their internal structure, trapped ions can also provide very accurate high-resolution clocks (Fisk, 1997). A linewidth of less than 0.001 Hz has been obtained in a trapped-ion clock (Fig. 6). The advantages of this very narrow linewidth are offset by the fact that trapped-ion experiments typically must use relatively few atoms because of attendant higher velocities (and Doppler shifts) associated with trapping large numbers. Therefore, the performance of the most accurate ion clocks is currently about equal to that of the best cesium clocks (Berkeland *et al.*, 1998).

The most accurate mass spectroscopy is now performed with ions in Penning ion traps (Ghosh, 1995). Ion mass ratios have been determined with an inaccuracy of about 1 part in 10^{10} by measuring the ratio the cyclotron frequencies for different mass ions in the same trap. Proton and antiproton masses have been measured to be equal at this level, providing the most stringent test of *CPT* invariance for baryons (Gabrielse *et al.*, 1998).

B. Inertial measurements with atom interferometers

Phase shifts arise when matter-wave interferometers accelerate, and atom interferometers have proved to be sensitive inertial sensors because such phase shifts generally vary with the mass and inversely with the velocity of the interfering particle (Adams *et al.*, 1994). Because of their high potential sensitivity, atom interferometers

are being developed for use as accelerometers, rotation sensors, gravimeters, and gradiometers.

The freely propagating matter waves in an interferometer form fringes with respect to an inertial reference frame. Hence, if the interferometer moves noninertially while the atoms are in transit, the fringes are shifted from the location where they would have been if the interferometer were stationary. For example, if the interferometer in Fig. 1 has acceleration upward, atom waves that pass through the (accelerating) middle grating at the same grating location shown in the figure will form fringes that will be observed a distance $D=a\tau^2$ below the centerline (where $\tau=L/v$ is the time for an atom moving with velocity v to travel the distance L between adjacent gratings). This displacement is observed as a phase shift

$$\varphi_{\text{acceleration}}=2\pi\left(\frac{-D}{d_g}\right)=-\frac{2\pi}{d_g}\left(\frac{L}{v}\right)^2 a=-\frac{2\pi m^2\lambda_{\text{dB}}A}{h^2}a, \tag{1}$$

where d_g is the period of the gratings, $\lambda_{\text{dB}}=h/mv$ is the de Broglie wavelength for an atom with mass m and velocity v, and $A=L^2(\lambda_{\text{dB}}/d_g)$ is the area enclosed by the paths of the interferometer. If the interferometer rotates with angular rate Ω, the resultant Coriolis acceleration $\vec{a}=2\vec{v}\times\vec{\Omega}$ gives rise to a rotational phase shift,

$$\varphi_{\text{rotation}}=\left[\frac{2\pi}{d_g}\left(\frac{L}{v}\right)^2 2v\right]\Omega=\left[4\pi\frac{mA}{h}\right]\Omega. \tag{2}$$

The second expression is the usual Sagnac phase shift. This phase shift exceeds that of a light interferometer with the same enclosed area by the ratio, $mc^2/\hbar\omega$, which can exceed 10^{10}.

Atom interferometers have already made dramatic improvements in measurements of phase shifts due to rotation and gravitation relative to earlier measurements with neutron and electron interferometers. Gravitational measurements with an accuracy approaching 10^{-9} g have been made using a laser-cooled-atom interferometer (Kasevich and Chu, 1991). Interferometers using an uncooled atomic beam have measured rotations with a sensitivity of 4 millidegree per hour in a 1 s measurement (Gustavson *et al.*, 1997; Lenef *et al.*, 1997), about 3 orders of magnitude better than measurements with neutron or electron interferometers.

Interferometric measurements of gravity confirm the weak equivalence principle. Orbiting atom interferometers might improve on this important null test. Similarly, orbiting atom rotation sensors should have the sensitivity to test the frame drag predictions of general relativity.

C. Measurements of atomic and molecular properties

Better determination of atomic properties is another one of the payoffs of the new techniques for atom manipulation. This has led to a more precise spectroscopic determination of many atomic energy levels. In addition, atom interferometers allow sensitive absolute measurements of the perturbations applied to atoms or molecules in one of the two arms. Examples are the determination of the electric polarizability of Na in its ground state (Fig. 7), and the measurement of the phase shift associated with passage of Na and Na_2 waves through a gaseous medium, essentially measuring the matter-wave index of refraction.

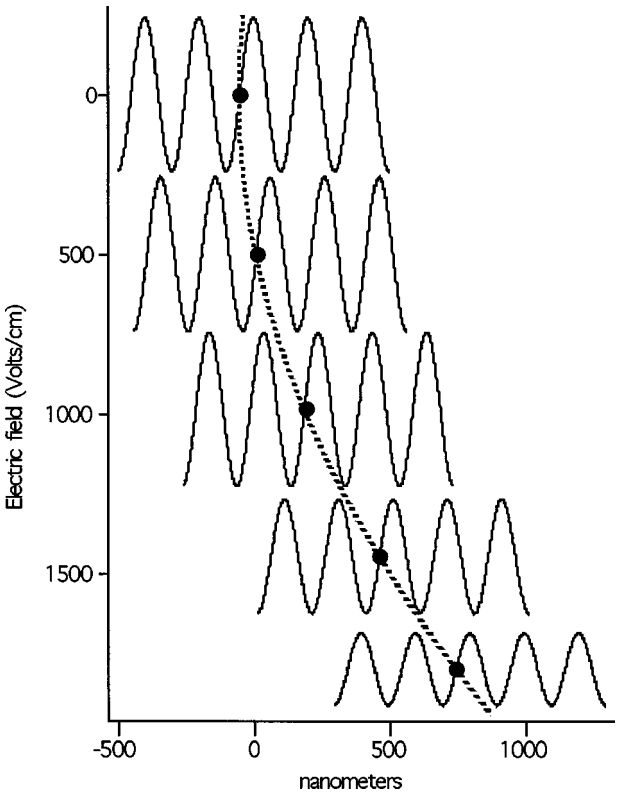

FIG. 7. The fringes in a separated-beam interferometer (shown in Fig. 1) shift in proportion to the Stark shift, $V_{\text{Stark}}=-1/2\alpha\mathbf{E}^2$, where α is the ground-state electric polarizability and $\mathbf{E}$ is the electric field applied to the sodium atoms in one side of the interferometer (Ekstrom *et al.*, 1995). The decrease of amplitude at larger phase shift reflects the finite coherence length of the beam. The quadratic fit (dashed line) allows 0.3% absolute determination of α. This exceeds the accuracy of the best theoretical calculations.

Neutral atom traps with their dense submillikelvin samples have revolutionized free-to-bound spectroscopy (also called photoassociative spectroscopy), in which an unbound atom pair is excited to a bound molecular state (Walker and Feng, 1994). The resolution, limited by the thermal energy of the free atoms, has been reduced from hundreds of inverse centimeters to 0.001 cm^{-1}, while the angular momentum of the colliding atoms, which determines the complexity of the molecular rotational spectra, has been reduced from hundreds of $\hbar$ to one or two. Consequently, extremely high-resolution free-bound spectra have been obtained with resolved hyperfine and rovibrational structure. For the first time it has become possible to study excited states very near to dissociation with corresponding internuclear separations of 2.5 to 10 nm. This has allowed the observation of pure long-range molecules—excited-state molecules

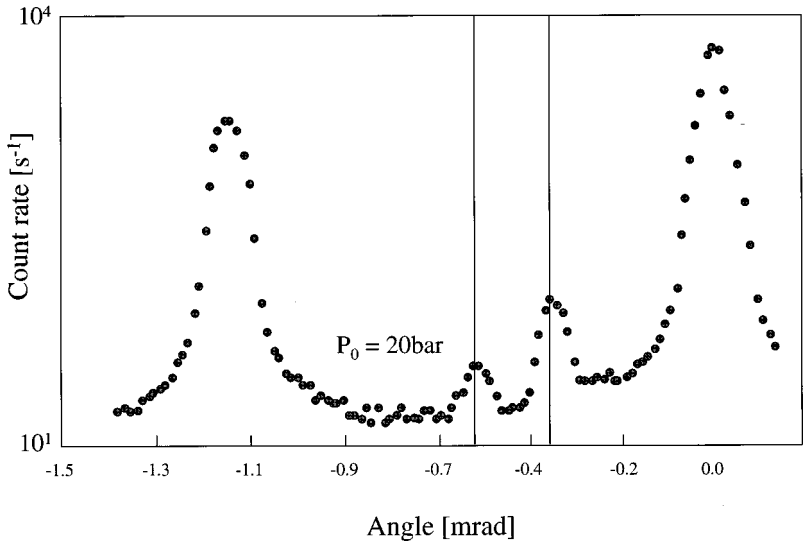

FIG. 8. Diffraction pattern for a helium cluster beam after passing through a transmission grating. The vertical lines indicate the peaks of the dimer (left) and trimer (right).

that have shallow (e.g., 1 K) well depths with inner potential barriers beyond 2.5 nm. The structure of these molecules is well described by theories based entirely on the properties of the separated atoms. Remarkably, free-bound spectroscopy has allowed determination of oscillator strengths for the important resonance transitions of Na, K, and Rb to 0.1%, better than they can be determined by any other technique. It has also provided improved determinations of the interatomic potentials, and corresponding improvements in the calculations of many atomic collision processes that depend on these potentials.

Extremely weakly bound molecules have been studied using nanofabricated structures. A diffraction grating was used to analyze a collimated beam from a supersonic expansion of cold He gas, showing the existence $^4He_3$ trimers and higher n-mers and conclusively demonstrating the existence of the $^4He_2$ dimer (Schollkopf and Toennies, 1996), which was previously thought not to be bound (Fig. 8). Subsequent measurements of the attenuation of $^4He_2$ by a nanofabricated sieve showed it to have an internuclear separation of 6.5 nm, making it by far the largest ground-state diatomic molecule and also the most weakly bound, with a dissociation energy of only 10^{-7} eV.

V. CONCLUSION

We have presented a brief summary of some of the novel techniques for manipulating atoms, and the measurements that these techniques have made possible. Probably the most exciting thing about this field is that many of these techniques have matured from research projects to useful tools only in the past few years. Thus the next decade promises to see an explosive growth of the manipulation and study of individual atoms at the quantum wave-packet level. This will allow many basic issues of quantum mechanics to be explored, and is also likely to give rise to a new generation of practical measurement devices that use the basic external and internal quantum properties of atoms.

REFERENCES

Adams, C., M. Sigel, and J. Mlynek, 1994, Phys. Rep. **240**, 143; provides a review of atom optics and atom interferometry.

Anderson, M. H., J. R. Ensher, M. R. Matthews, C. E. Wieman, and E. A. Cornell, 1995, Science **269**, 198; a bibliography of about 600 papers on BEC in dilute gases can be found online at http://amo.phy.gasou.edu/bec.html/bibliography.html.

Andrews, M. R., C. G. Townsend, H.-J. Miesner, D. S. Durfee, D. M. Kurn, and W. Ketterle, 1997, Science **275**, 637.

Atomic Physics, 1980–1996, Vols. 7–15, *Proceedings of the International Conference on Atomic Physics*; has many articles covering the topics discussed in this article.

Bergquist, J., 1996, Ed., *Proceedings of the Fifth Symposium on Frequency Standards and Metrology*, Woods Hole, Massachusetts, 1995 (World Scientific, Singapore).

Berkeland, D. J., J. D. Miller, J. C. Bergquist, W. M. Itano, and D. J. Wineland, 1998, Phys. Rev. Lett. **80**, 2089.

Berman, P. R., 1997, *Atom Interferometry,* Suppl. 3 Adv. At. Mol. Phys. (Academic, San Diego, CA, 1997).

Blatt, R., and P. Zoller, 1988, Eur. J. Phys. **9**, 250.

Bollinger, J. J., W. M. Itano, D. J. Wineland, and D. J. Heinzen, 1996, Phys. Rev. A **54**, R4649.

Cirac, J. I., and P. Zoller, 1995, Phys. Rev. Lett. **74**, 4091.

Cohen-Tannoudji, C., and W. D. Phillips, 1990, Phys. Today **43**, 33.

Davis, K. B., *et al.*, 1995, Phys. Rev. Lett. **75**, 3969.

Dehmelt, H., 1995, Science **247,** 539.

Einstein, A., 1924, Sitzungsber. K. Preuss. Akad. Wiss., Phys. Math. K1. **1924**, 261.

Einstein, A., 1925, Sitzungsber. K. Preuss. Akad. Wiss., Phys. Math. K1. **1925**, 3.

Ekert, A., and R. Jozsa, 1996, Rev. Mod. Phys. **68**, 733.
Ekstrom, C. J., J. Schmiedmayer, M. S. Chapman, T. D. Hammond, and D. E. Pritchard, 1995, Phys. Rev. A **51**, 3883.
Fisk, P. T. H., 1997, Rep. Prog. Phys. **60**, 761.
Gabrielse, G., D. Phillips, W. Quint, H. Kalinowsky, G. Rouleau, and W. Jhe, 1995, Phys. Rev. Lett. **74**, 3544.
Ghosh, P. K., 1995, *Ion Traps* (Clarendon, Oxford); and Bergström, I., C. Carlberg, R. Schuch, Eds., 1995, *Proceedings of the Nobel Symposium on Trapped Charged Particles and Related Fundamental Physics*, Lysekil, Sweden, 1994, Physica Scr. **59**, both provide extensive discussions of ion traps and work that has been done with them.
Greytak, T., 1995, in *Bose-Einstein Condensation,* edited by A. Griffin, D. Snoke, and S. Stringari (Cambridge University, Cambridge, England).
Gross, E. P., 1961, Nuovo Cimento **20**, 454.
Gross, E. P., 1963, J. Math. Phys. **4**, 195.
Gustavson, T. L., P. Bouyer, and M. A. Kasevich, 1997, Phys. Rev. Lett. **78**, 2046.
Itano, W. M., *et al.*, 1998, Science **279**, 686.
Jin, D., C. E. Wieman, and E. A. Cornell, 1997, Phys. Rev. Lett. **78**, 764.
Kasevich, M., and S. Chu, 1991, Phys. Rev. Lett. **67**, 181.
Kasevich, M., and S. Chu, 1992, Appl. Phys. B **54**, 321.
Keith, D. W., M. L. Shattenburg, H. I. Smith, and D. E. Pritchard, 1988, Phys. Rev. Lett. **61**, 1580.
Ketterle, W., and N. J. van Druten, 1996, Adv. At., Mol., Opt. Phys. **37**, 181.
Leibfried, D., T. Pfau, and C. Monroe, 1998, Phys. Today **51**, 22.
Lenef, A., T. D. Hammond, E. T. Smith, M. S. Chapman, R. A. Rubenstein, and D. E. Pritchard, 1997, Phys. Rev. Lett. **78**, 760.
Luo, F., C. F. Giese, W. R. Gentry, 1996, J. Chem. Phys. **104**, 1151.
Metcalf, H., and P. van der Straten, 1994, Phys. Rep. **244**, 203; a review of laser cooling and trapping of neutral atoms.
Meystre, P., and S. Stenholm, Eds. 1985, J. Opt. Soc. Am. B **2**, 1706; a special issue on the mechanical effects of light.
Mitchell, T. B., J. J. Bollinger, D. H. E. Dubin, X.-P. Huang, W. M. Itano, and R. H. Baughman, 1998, Science **282**, 1290.
Monroe, C., W. Swann, H. Robinson, and C. Wieman, 1990, Phys. Rev. Lett. **65**, 1571.
Monroe, C., and J. Bollinger, 1997, Phys. World **10**, 37.
Morinaga, M., M. Yasuda, T. Kishimoto, F. Shimizu, 1996, Phys. Rev. Lett. **77**, 802.
Newbury, N. R., and C. E. Wieman, 1996, Am. J. Phys. **64**, 18, is an extensive bibliography on neutral atom trapping.
Phys. Today 1997, **50**, 17.
Pitaevskii, L. P., 1961, Sov. Phys. JETP **13**, 451.
Pritchard, D. E., 1991, in *Atomic Physics* 12, Proceedings of the 12th International Conference on Atomic Physics, edited by Jens C. Zorn and Robert L. Lewis (AIP, New York) p. 165.
Raab, E. L., M. Prentiss, A. Cable, S. Chu, and D. E. Pritchard, 1987, Phys. Rev. Lett. **59**, 2631.
Schollkopf, W., and J. Toennies, 1996, J. Chem. Phys. **104**, 1155.
Simon, E., P. Laurent, C. Mandache, and A. Clairon, 1997, in Proceedings of the *11th European Frequency and Time Forum* (Swiss Foundation for Research in Microtechnology, Neuchâtel, Switzerland), p. 43.
Stamper-Kurn, D. M., M. R. Andrews, A. P. Chikkatar, S. Inouye, H.-J. Miesner, J. Stenger, and W. Ketterle, 1998, Phys. Rev. Lett. **580**, 2027.
Steane, A., 1998, Rep. Prog. Phys. **61**, 117.
Thywissen, J. H., K. S. Johnson, R. Younkin, N. H. Dekker, K. K. Berggren, A. P. Chu, M. Prentiss, and S. A. Lee, 1997, J. Vac. Sci. Technol. B **15**, 2093.
Walker, T., and P. Feng, 1994, Adv. At., Mol., Opt. Phys. **34**, review ultralow-temperature collision studies.
Walther, H., 1993, Adv. At., Mol., Opt. Phys. **31**, 137.
Wieman, C., and S. Chu, Eds. 1989, J. Opt. Soc. Am. B **6**, 2020; a special issue with many articles on laser cooling.
Wineland, D. J., and W. M. Itano, 1987, Phys. Today **40**, 34.